A Simplified Thermal Analysis of an Inductively Heated Casting Furnace

Randy Clarksean
and
Charles Solbrig
Technology Development Division
Argonne National Laboratory
-P.O. Box 2528
Idaho Falls, Idaho 83403

A paper submitted to the
1995 International Mechanical Engineering Congress and Exposition
San Francisco, CA
November 12-17

Abstract

A simplified thermal analysis technique was developed to analyze an inductively heated casting furnace. Initial operation of the vacuum casting furnace indicated that the outer shell of the vessel was exceeding the temperature design limit. The casting furnace is very complex and not easily modeled in a short period of time through the use of general purpose heat transfer codes. The model took into consideration conduction, natural convection, phase change, radiation heat transfer, and induction heating. The furnace was constructed from ceramic materials, stainless steel, copper, graphite, and other materials. To develop a model based on first principles within a couple of weeks was not considered possible. The alternate approach was to develop a simplified numerical model that relied heavily on experimental data. The purpose of the model was to accurately predict the maximum vessel shell temperatures. A basic 5 node transient model was developed for the complete system. The resultant model predicted the transient heatup of the casting furnace and was able to predict the maximum shell temperature to within 5 °C. The model was also capable of predicting the effect of

different operations on the shell temperature. This type of modeling approach can be used to troubleshoot existing heat transfer equipment problems, study the effect of different operating sequences, and give insight into the redesign of similar equipment.

1 Introduction

The modeling of heat transfer equipment is a complicated task. The types of effects that can be considered include conduction, convection, radiation, laminar or turbulent flow, phase change (evaporation, condensation, solidification, or melting), multiple phases, direct contact of fluids, combustion processes, chemical reactions, etc. The situation may call for either transient or steady-state simulations. The current capabilities of commercially available analysis tools (such as FIDAP, FLUENT, FLOW3D, etc.) allow multiple phenomena to be considered in the modeling process. As more physical phenomenon are included in these models, the solution of the problem becomes more demanding numerically. These modeling efforts can quickly become very time consuming and expensive.

The modeling approach presented here takes into account several different physical phenomenon, but does not attempt to model the exact details of each phenomena. Rather, the approach is to use a simplified model that relies on experimental data to assist in the model development. The use of experimental data and the knowledge of the heat transfer mechanisms can allow the simplified approach to correctly model a complex system. This type of modeling approach has its limitations, but can be useful for engineering applications where a quick answer is needed to assist in day-to-day operations of heat transfer equipment. The technique is applied here to an inductively heated casting furnace.

Inductively heated casting furnaces are commonly used for industrial or research applications (Reference [1]). These furnaces are used for melting and casting a variety of metals. Some of the advantages of inductively heated furnaces include fast melt times, freedom from gases which may cause undesirable metallurgical reactions, low operating costs, reduced metal loss, and automatic stirring. At Argonne National Laboratory, an inductively heated

casting furnace has been used for casting metal fuel pins (uranium alloy) for the Experimental Breeder Reactor II (EBR-II). In the future, the furnace will be used for the development and casting of a metal waste form. The metal waste form is an end product from the treatment of the EBR-II spent fuel.

A schematic of the casting furnace operated at Argonne is shown in Figure 1. The major components of the inductively heated vacuum casting furnace are the coils, crucible, mold pallet region, vessel (shell), and power supply (not shown). An alternating current is fed to the induction coils. The flow of current through the coils induces a voltage field in the material around the coil. The induced field causes an eddy current to dissipate within the material. The end result of the induced current flow is the generation of heat in the material. Typically, the heating principally occurs in the outer layer of the material being heated (skin-effect). The amount of heat generated in a material depends on the electrical properties of the material and the power supply frequency.

There are no cooling coils in the furnace. Heat loss from the system is predominantly passive, with some flow from a ventilation system blowing on the outside of the vessel, which aids in heat removal by convection. The furnace was designed to maintain the crucible and its contents at 1560°C. In order to achieve this temperature, a 30 kW power supply was required. The outer pressure vessel, referred to as the shell, was designed for a maximum of 6.8 atmospheres pressure (100 psig) and 316°C (600°F).

2 Problem Definition

The general operating cycle for the furnace is shown in Figure 2. The four general phases of the cycle are heatup, dissolution, mixing, and casting. During the heatup phase, the power supply is at maximum power, approximately 30 kW. The casting crucible and the material it contains is being heated rapidly to reach the dissolution phase. Note that the rate of temperature rise of the crucible slows for a short time as the uranium in the crucible changes from a solid to a liquid. The power input to the casting furnace decreases as the uranium

melts because of decreased coupling between the coils and the molten material results in less total energy being deposited in the furnace.

The dissolution phase starts when the crucible reaches a temperature of 1560°C. The alloys previously cast included U-Zr and U-Pu-Zr. The crucible temperature is maintained for a fixed period of time to insure that all of the zirconium is "dissolved" by the molten uranium, or uranium and plutonium. While the crucible is maintained at 1560°C, the components surrounding the crucible region are being heated up. This heating results in a slow decrease in the average power requirements for the casting furnace. Analysis of the power data shown in Figure 2 indicates that the power requirements are slowly decreasing.

The third phase of the cycle is mixing. One advantage of induction heating is that the molten material is mixed. The mixing is the result of the fields induced in the molten material by the coils. The induced field can cause the molten metal to flow inside the crucible. Mixing is facilitated in this furnace by cycling between 0 and 100 percent of maximum power. The cycling allows the maximum flow to occur for short periods of time and prevents excessive crucible and shell temperatures.

The last phase of the operating cycle is casting. After mixing is complete, the crucible is maintained at a constant temperature prior to casting. The hold temperature is selected to insure that high quality fuel pins are obtained during the cast. Quartz molds are lowered into the melt, the furnace pressure is rapidly increased, and as a result of this pressurization, the molten alloy flows into the molds and solidifies. This ends the casting cycle.

The qualification process required several stages of testing. The casting furnace was designed to be operated remotely in a hot cell at Argonne. Operating in this type of environment requires a thorough qualification process to demonstrate that the equipment can be operated and maintained through the use of telerobotic manipulators and cranes. Before the equipment is placed in the hot cell and tested there is extensive testing outside the hot cell to insure that the equipment can be assembled, operated, and maintained remotely. The out-of-cell testing was restricted to lower operating temperatures to insure personnel safety

and to progressively test the capabilities of the furnace at increasing temperature levels. These lower temperatures prevented the furnace from being tested at its normal operating temperature.

Once the out-of-cell testing was completed, the casting furnace was placed inside the hot cell for final qualification. Part of the qualification process for the casting furnace required the casting of depleted uranium (U^{238}) fuel pins. This test was the first complete test of the casting furnace. Near the end of the dissolution phase, the lower region of the vessel started to approach 316°C, the design limit. The test was stopped before the shell temperature exceeded the design limit.

The potential for a shell temperature exceeding the design limit prevented further operations. A quick estimate of the maximum expected shell temperature was needed to determine if excessive stresses existed in the shell. If excessive stresses occurred, the pressure rating of the shell would have to be changed.

3 Model Development

A method of determining the maximum shell temperature was needed to determine if casting operations could continue. Thus the objective of this work was to develop a model quickly that could use existing experimental data to accurately predict maximum temperatures, or if the temperatures were unacceptably high, to find what modifications were required to allow further casting furnace operations.

The casting furnace is a very complicated piece of equipment. Many different materials are used including graphite in the crucible, quartz in the molds, stainless steel in the shell and vessel base, and copper in the coils. The inductive heat is deposited principally in the graphite crucible, but some of it is also absorbed by the shell. Analysis with a commercial heat transfer code was initially considered, but was discarded because of the time required to develop the input, the difficulty of representing inductive heating in such a code, and the difficulty of being able to determine what input variables would have to be modified to match

the existing experimental data. Instead, it was decided to develop a simplified lumped mass model which had very few input variables.

The schematic of the casting furnace shown in Figure 1 suggests a representation consisting of the following five nodes; 1) the casting crucible and casting charge (ie, the metal to be cast, 2) the shell upper section, 3) the shell lower section, 4) the pallet, and 5) the vessel base. Five locations were also dictated by the five available thermocouples. The masses and other properties associated with each node were initially estimated, but the final values used were adjusted to provide satisfactory agreement with the test data.

Figure 3 shows a schematic of the heat transfer paths associated with each of the five nodes. The heat transfer paths considered as significant are the following. The crucible node receives heat by induction and loses it by radiation and convection. The physical structure supporting the crucible is small, allowing conduction to be neglected. The lower shell receives heat by radiation and convection from the crucible, loses heat by conduction to the upper shell ($sh1$) and the vessel base (vb), and loses heat to the environment by convection. Radiation to the environment is neglected because it would be small. The upper part of the shell receives heat from the crucible by radiation and convection, by conduction from the lower shell, and loses heat to the pallet by conduction and the environment by convection. The pallet receives heat from the upper shell by conduction and loses heat by convection to the environment. The only heat transfer mechanism to the vessel base is taken as conduction from the lower shell. The vessel base is considered to include part of the floor which it rests on so that conduction to the floor is neglected.

The heat balance on the crucible is approximated as

$$\frac{d(mi)}{dt} = q(t) - h^* A_{cr}(T_{oc} - T_{sh2}) \tag{1}$$

where

A_{cr} = *crucible surface area.*

i = *enthalpy.*

h^* = *effective heat transfer coefficient.*

m = *mass,* $m_{cr} + m_{melt}$.

m_{cr} = *effective mass of crucible.*

m_{melt} = *mass of casting charge.*

$q(t)$ = *rate of heat addition by induction heating.*

t = *time.*

T_{oc} = *effective outer coil region temperature.*

T_{sh2} = *lower shell temperature.*

Initially, Equation 1 was written with T_{oc} replaced with T_{cr}. Analysis of the experimental data indicated that T_{cr} was not the correct driving force for energy transport from the crucible region to the shell. Figure 1 shows the crucible surrounded by an insulator and the induction coils. The temperature of the coils, or coil region, is more appropriate for the driving force for the transfer of energy from the crucible node to the nodes on the shell. The driving force temperature was defined as

$$T_{oc} = PT \cdot (T_{cr} - T_{sh2}) + T_{sh2} \tag{2}$$

where PT is a ratio to take into account the fact that the shell is actually receiving radiation and natural convection from the coil region which is at a lower temperature than the crucible. PT was determined to be 0.42 through the analysis of the experimental data. This value is physically realistic because it gave a maximum coil region temperature of 800 to 900°C. This is realistic because the ceramics behind the coil are probably above this temperature, and the coils are probably at a maximum temperature of 600 to 700°C.

The radiative and convective transport to the shell primarily depends on T_{sh2}. Less energy directly reaches the upper shell because of the crucible covers and separation of the upper and lower vessel (see Figure 1). Because the majority of the energy is transported to the lower shell, it is reasonable to let the heat transfer from the crucible depend only on T_{sh2}.

The rate of heat addition due to induction heating, $q(t)$, was based on the maximum output of the power supply and engineering judgement. The induced voltage field from the current flow through the coils can cause heating in any of the surrounding materials. Materials that are not good electrical conductors will not be heated inductively, but the stainless steel shell will be inductively heated. Past experience indicates that approximately 80 to 90 percent of the power will heat the crucible and casting charge. The remaining energy was assumed to heat the upper and lower shell. The effective heat transfer coefficient, h^*, includes both radiation and convection and is written as

$$h^* = h_{nc} + h_{rad} \tag{3}$$

where the subscripts nc and rad refer to natural convection and radiation respectively.

The analytical for of the natural convection portion of h^* was assumed to be that of a typical natural convection heat transfer correlation for high Ra conditions. For a high Ra the Nu relationship depends on the 1/3 power of the Ra. This gives

$$Nu = \frac{h_{nc}L}{k} = a\ Ra^{1/3} \tag{4}$$

where

$$\begin{aligned} a &= constant\ coefficient. \\ Ra &= Rayleigh\ number. \\ &= \left(\frac{g\beta}{\nu^2}\right) PrL^3\Delta T \end{aligned}$$

g = *gravity.*

k = *fluid thermal conductivity.*

L = *characteristic length.*

Nu = *Nusselt number.*

Pr = *Prandtl number.*

β = *coefficient of thermal expansion.*

ΔT = *temperature driving force.*

$= (T_{oc} - T_{sh2})$.

ν = *kinematic viscosity.*

Substituting the Ra definition into Equation 4 and rearranging gives

$$\begin{aligned} h_{nc} &= a\left(\frac{k}{L}\right) Ra^{1/3} \\ &= a\left(\frac{k}{L}\right)\left[\left(\frac{g\beta}{\nu^2}\right) PrL^3\Delta T\right]^{1/3} \\ &= D\left(\frac{g\beta}{\nu^2}\right)^{1/3} \Delta T^{1/3} \end{aligned} \tag{5}$$

The quantity $\left(\frac{g\beta}{\nu^2}\right)^{1/3}$ is not grouped into D because it varies by over two orders of magnitude for the temperature range of interest. The remaining terms are lumped into one approximately constant term D because the variation of these terms is much less.

For the radiative portion of the effective heat transfer coefficient, a simple radiative flux can be written as

$$\begin{aligned} q_{rad} &= A_{cr}\epsilon\sigma(T_{oc}^4 - T_{sh2}^4) \\ &= A_{cr}h_{rad}(T_{oc} - T_{sh2}) \end{aligned} \tag{6}$$

where

$$
\begin{aligned}
h_{rad} &= \epsilon\sigma(T_{oc}+T_{sh2})(T_{oc}^2+T_{sh2}^2) \\
\epsilon &= effective\ emissivity\ of\ the\ coil\ region. \\
\sigma &= Stefan-Boltzmann\ constant.
\end{aligned}
$$

Substituting h_{nc} and h_{rad} into Equation 3 gives the final definition of the effective heat transfer coefficient.

$$h^* = D\left(\frac{g\beta}{\nu^2}\right)^{1/3}\Delta T^{1/3} + \epsilon\sigma(T_{oc}+T_{sh2})(T_{oc}^2+T_{sh2}^2) \tag{7}$$

The unique approach to this problem is the process used to obtain constants in Equation 1. There are actually two unknown constants in Equation 1. The unknowns are m_{cr}, the mass of the crucible node, and the constant D in the effective heat transfer term. The mass, m_{cr}, is considered unknown because some type of definition must be made on how large of a region should be associated with the crucible node.

Typically in model development, the modeler selects and defines the size of each node. Properties for each of these nodes must be defined within the model. For a complex system like the casting furnace, 10^3 to 10^4 nodes would be required to accurately model the heat transfer. With the simplified model the difficulty is in the selection of the representative properties for each node. Each node may represent several materials which may have a large variation in material properties. Through the use of experimental data, these constants can be selected based on the design of the model.

The effective crucible mass, m_{cr}, and constant D can be determined at different phases of the casting cycle. During the dissolution phase, the crucible temperature is held constant. This allows Equation 1 to be rewritten as

$$\frac{d(mi)}{dt} = 0 = q(t) - h^*A(T_{cr}-T_{sh2}) \tag{8}$$

Using data from the dissolution phase allows D to be determined without having to determine m_{cr} simultaneously. Rearranging Equation 8 and substituting for h^* gives

$$D = \frac{q(t)/A(T_{oc} - T_{sh2}) - \epsilon\sigma(T_{oc} + T_{sh2})(T_{oc}^2 + T_{sh2}^2)}{(g\beta/\nu^2)^{1/3}\Delta T^{1/3}} \tag{9}$$

The terms on the right hand side of Equation 9 can be determined from the experimental data, which allows the calculation of the constant D.

The next constant to be determined is the effective mass of the crucible node, m_{cr}. During the heatup phase of the casting cycle, the crucible temperature and the power requirements are known. In addition, the rate of heat transfer from the crucible region to the shell can be calculated through the use of h^*. Approximating Equation 1 numerically as

$$\frac{(mi^n - mi^{n-1})}{\Delta t} \approx q(t) - h^* A(T_{cr}^{n-1} - T_{sh2}^{n-1}) \tag{10}$$

where the superscripts refer to time steps of Δt. The left hand side of this equation can be rewritten as

$$mi^n - mi^{n-1} = (m_{cr}i_{cr}^n + m_{melt}i_{melt}^n) - (m_{cr}i_{cr}^{n-1} + m_{melt}i_{melt}^{n-1}) \tag{11}$$

but for the experimental case where $m_{melt} = 0$, Equation 10 can be manipulated to give m_{cr}.

$$m_{cr} = \frac{\Delta t(q(t) - h^* A(T_{oc}^{n-1} - T_{sh2}^{n-1}))}{(i_{cr}^n - i_{cr}^{n-1})} \tag{12}$$

The empirically determined value of m_{cr} was approximately twice the actual weight of the graphite crucible. The higher weight is reasonable when one considers the weight of the surrounding coils, supports, and ceramic insulator. For a simplified model, this was considered to be good agreement.

The energy equations for the remaining nodes were developed from a simple circuit analogy, such as discussed in Reference [2]. The heat transfer mechanisms considered were conduction from adjacent nodes, natural convection and radiation from the crucible region,

natural convection from the outer surface of the vessel, and induction heating. Phase change of the casting charge, or melt, was taken into account through i_{melt}.

$$
\begin{aligned}
m_{sh2}C_p\frac{dT_{sh2}}{dt} &= PS\ h^*A_{cr}(T_{oc}-T_{sh2}) - \frac{(T_{sh2}-T_{sh1})}{R_1} \\
&\quad -\frac{(T_{sh2}-T_{vb})}{R_2} - h_\infty A_{sh2}(T_{sh2}-T_\infty) + PS\ q_{sh}(t) \qquad (13)\\
m_{sh1}C_p\frac{dT_{sh1}}{dt} &= (1-PS)h^*A_{cr}(T_{oc}-T_{sh2}) - \frac{(T_{sh1}-T_{sh2})}{R_1} \\
&\quad -\frac{(T_{sh1}-T_{pal})}{R_3} - h_\infty A_{sh1}(T_{sh1}-T_\infty) + (1-PS)q_{sh}(t) \qquad (14)\\
m_{vb}C_p\frac{dT_{vb}}{dt} &= \frac{(T_{sh2}-T_{vb})}{R_2} \qquad (15)\\
m_{pal}C_p\frac{dT_{pal}}{dt} &= \frac{(T_{sh1}-T_{pal})}{R_3} - h_\infty A_{pal}(T_{pal}-T_\infty) \qquad (16)
\end{aligned}
$$

where T_∞ is the ambient temperature and q_{sh} is the amount of induction heating in the shell.

The conductive resistances, R_1 to R_3, were originally estimated from cross sectional areas, thermal properties, and distances between the nodes. These estimates were then heuristically modified to match the temperatures from an empty crucible casting batch. Modification was necessary because the effective conductive path for each node is not known in advance and the effect of natural convection and radiation heat transfer from portions of one node to another are not known in advance.

Similarly, the mass of each node was also estimated from the data. Each of the individual masses could be modified during the determination of the constants, but the total mass of the system was maintained at a constant value. Maintaining the total mass as a constant allows the total thermal mass of the system to be taken into account, which is important for a realistic transient solution.

The term PS is the percent of energy transported from the crucible to the lower shell region, $sh2$. Approximately 80 percent of the energy is transported to the lower shell, and the remaining 20 percent reaches the upper shell. Less energy directly reaches the upper shell because of the crucible covers and separation of the upper and lower vessel (see Figure 1).

Because the majority of the energy is transported to the lower shell, it is reasonable to let the heat transfer from the crucible depend only on T_{sh2}.

4 Discussion of Results

4.1 Model Validation

The model constants were determined from an empty crucible test, which is not described here. The constants obtained from the empty crucible test were then used to predict temperatures for a depleted uranium casting (discussed here). The depleted uranium casting was stopped before the dissolution phase was completed because the lower shell temperature would have exceeded 316°C (600°F), as discussed in Section 2. The predicted and measured temperatures are shown in Figures 4 and 5.

The addition of the depleted uranium mass to the crucible did not noticeably affect the predicted crucible temperature (Figure 4) from that of the empty crucible test. There is a slight bend in the crucible temperature rise which represents the uranium phase change. The model predicted a slightly shorter time to reach the dissolution temperature of 1560°C, but in general showed good agreement to the measured data.

The shell temperatures are shown in Figures 4 and 5. Figure 5 shows only the shell temperatures, which indicates that the model over predicts the maximum shell temperature. An overprediction of the shell temperature was acceptable because an estimate of the maximum temperature, or the stress induced by this temperature, was all that was needed for pressure derating of the vessel. Initially, the model predicts a more rapid heatup of the shell than experienced experimentally. The overprediction can be due to the assumed amount of induction heating and an overprediction of the energy transport from the crucible.

The model initially assumes 20 percent of the total power is deposited in the shell. Once the material in the crucible starts to undergo phase change, a higher percentage of the power goes into the melt and crucible, reducing the amount of energy that goes into the shell to 10

percent. These estimates were based on operating experience of a similar casting furnace, and are reasonable estimates. The amount of energy deposited in the shell will increase as the temperature of the shell increases. The increase is the result of the resistivity of the shell increasing. As the resistivity of the shell increases, the energy generated by the induced fields increases. For a shell temperature increase from 20°C to 315°C, the amount of induction heating increases by 40 percent.

The amount of energy transported from the crucible to the shell could also be overpredicted during the heatup phase of the cycle. The overprediction could be due to the determination of the coefficient D during the dissolution phase. The crucible and shell are at much higher temperatures during the dissolution phase, which could lead to an overprediction of the value of D for lower temperatures.

Overall, the agreement between the model and test results was found to be acceptable.

4.2 Application to Casting Cycle

The model was then used to predict the casting furnace temperatures for a complete casting cycle. The predicted maximum shell temperature was used to develop a safety case to allow continued operations at shell temperatures in excess of 316°C.

The predicted and measured temperatures are shown in Figures 6 and 7. As before, the numerical model predicts a shorter time to reach the dissolution temperature. This results in the mixing cycle starting at an earlier time. The predicted duration of the mixing cycle is longer than the measured time for the mixing cycle. The difference between the durations could be due to the location of the thermocouple in the casting furnace. The thermocouple is located in a thermocouple well in the center of the crucible. The mass located near this thermocouple can cool much more rapidly than the lumped mass of the crucible node in the model. The crucible node in the model accounts for a much larger mass. For this reason the thermocouple will respond much more quickly than the crucible node in the model. This is particularly true for short duration transients.

The intent of the model was to predict the maximum shell temperature for a complete casting cycle. As shown in Figure 7 the model met its objective. The maximum shell temperature was predicted within 5°C. The model overpredicted the initial shell heatup, but the temperatures during this time were only of secondary interest.

4.3 Model Utility

Once the model was found to successfully predict temperatures associated with the operation of the casting furnace, it was used to study the effect of different parameters on operations. The examination included a study of the effect of the number of mixing cycles on the maximum shell temperature or casting cycle duration. A change in the alloy was also examined.

The problem that initially caused the shell heating problem was excessive induction heating of the shell. It is common for induction heating system designs to be based on rules of thumb or simplified one-dimensional calculations. The uncertainty in these types of calculations can easily range from ±10 to 20 percent. An uncertainty of this size is reasonable if there is a cooling system for the furnace. The coils of the furnace can be water cooled, or the coils may be exposed to the environment, which would allow for natural convection and radiation heat transfer to the surroundings. In the present furnace there is no forced water cooling system. In this instance, any error in estimating the induction heating can have a more significant effect because heat is not as easily removed from the system.

Figures 8 and 9 show the effect of a 10 percent error in the distribution of the induction heating. The cycle time increases from approximately 7500 to 9700 seconds (29 percent increase). The maximum shell temperature increased from approximately 326°C to 403°C (26 percent increase in temperature rise). The cycle time and shell temperatures increase as a result of less heat entering the melt and more heat being deposited in the shell.

A small change in the amount of induction heating going into the crucible and the melt greatly impacts the operation of the casting furnace. The effect of induction heating would have to be carefully considered in a redesigned furnace, or if operations of the present furnace

were modified.

5 Conclusions

A simplified thermal model was developed to predict the maximum shell temperature of an inductively heated casting furnace. The model was unique because it relied on experimental data to correctly represent constants within the model. The determination of a limited set of constants allowed the five node model to correctly account for conduction, radiation heat transfer, natural convection, and phase change of the casting charge. The model was successful in predicting the maximum shell temperature. The model was also capable of predicting what effect the changes in process variables could have on the overall operation.

This type of modeling approach can also provide useful information related to redesign of heat transfer equipment. The model for this application was able to determine that maximum shell temperature is sensitive to small changes in the amount of induction heating that occurs in the crucible. An error of 10 percent in estimating the induction heating, can lead to an 26 percent increase in shell temperature.

Acknowledgements

This work was supported by the U.S. Department of Energy, Nuclear Energy Programs, under contract no. W-31-109-ENG-38.

References

[1] Davies, E.J., Conduction and Induction Heating, Peter Peregrinus Ltd., London England, 1990.

[2] Kreith, F., and Black, W., Basic Heat Transfer, Harper and Row Publishers, New York, 1980.

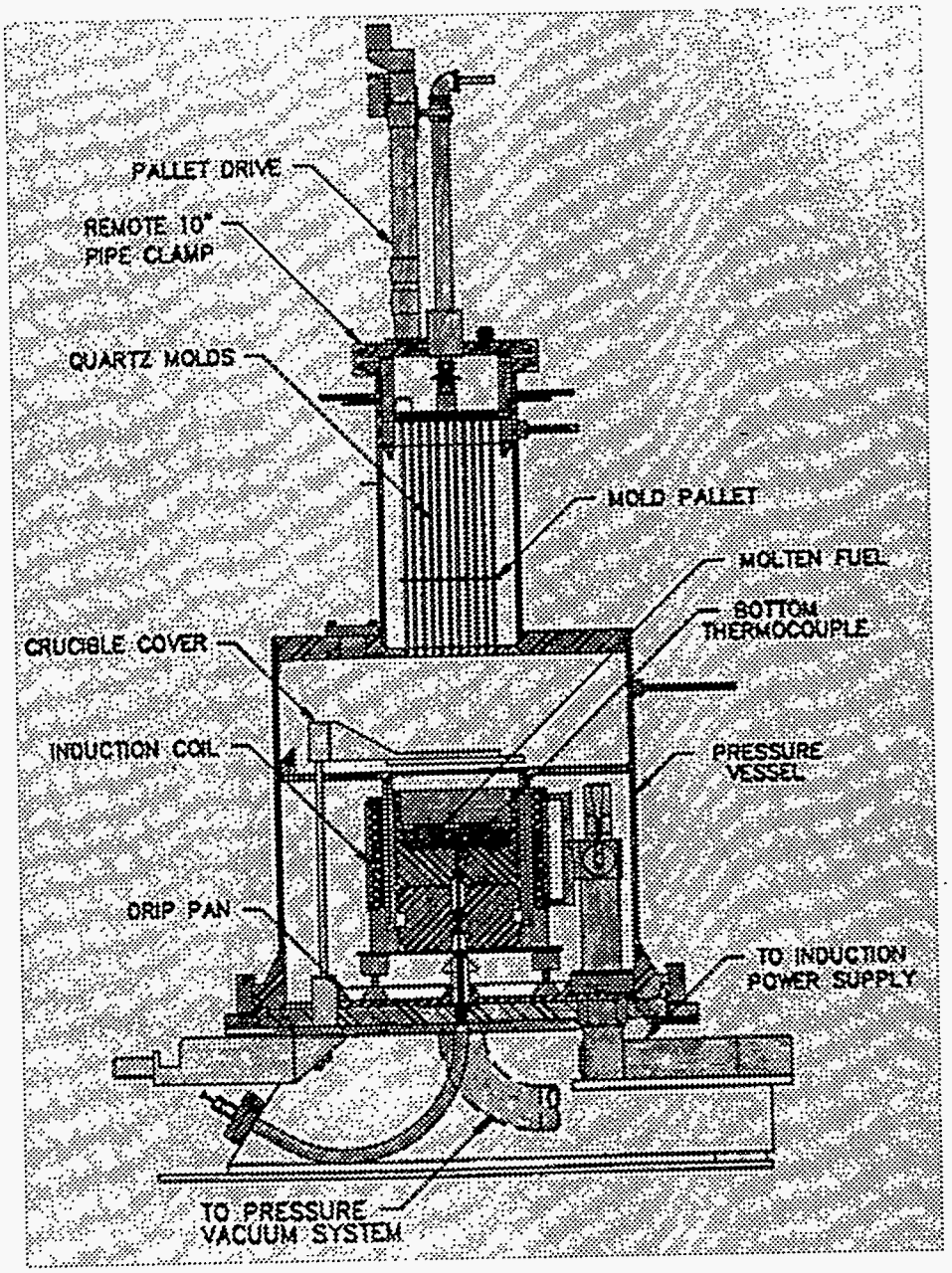

Figure 1: Schematic of inductively heated casting furnace.

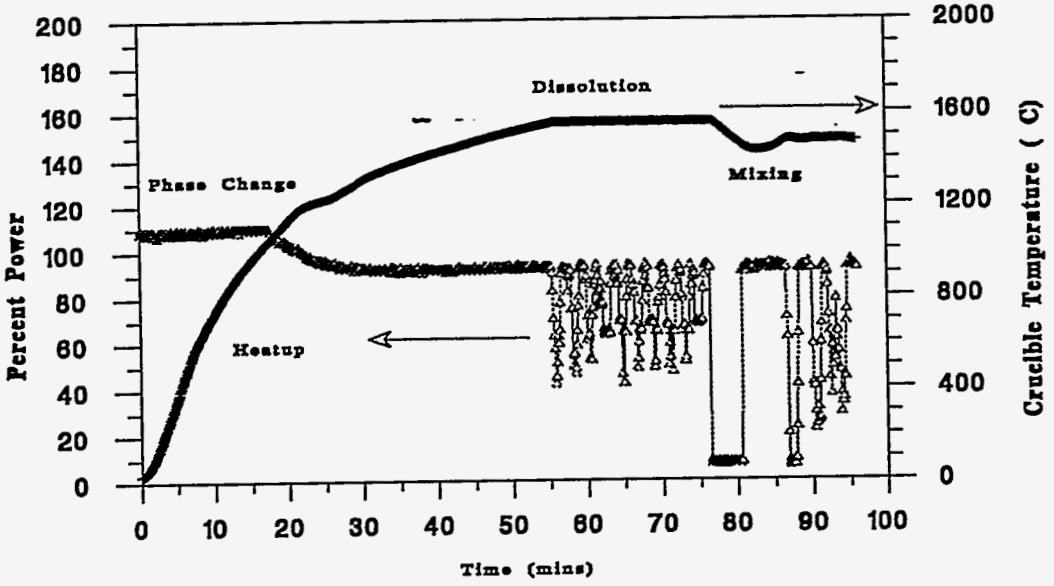

Figure 2: Typical casting furnace operating cycle.

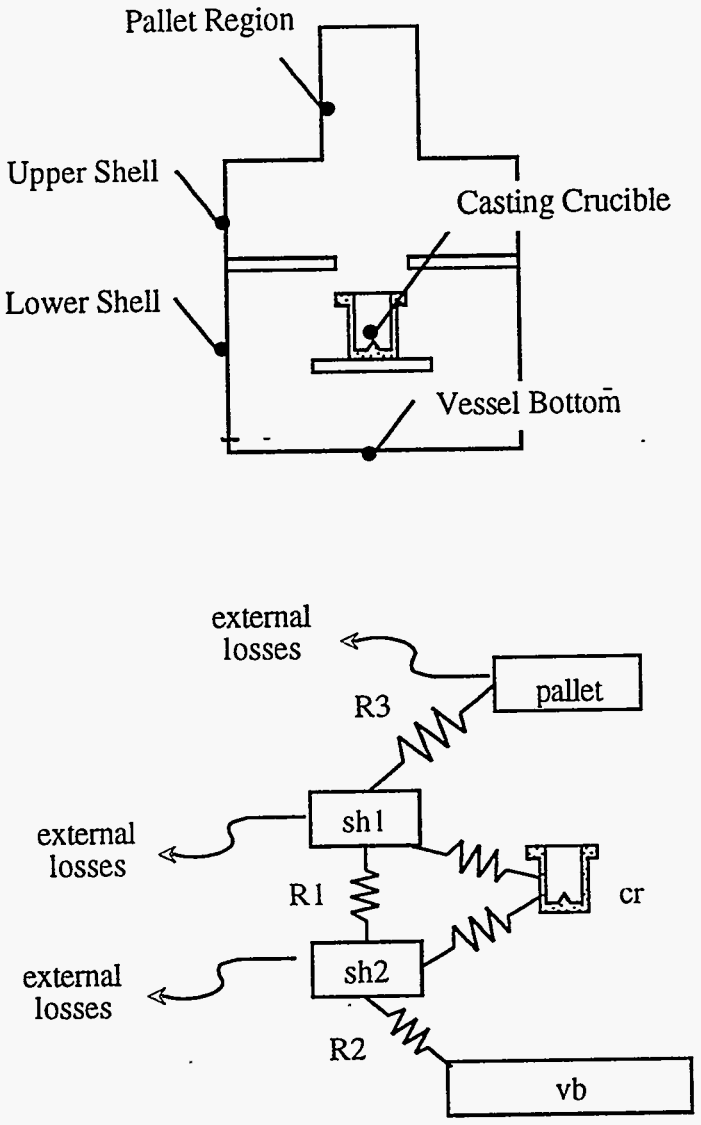

Figure 3: Nodal points for the simplified thermal model.

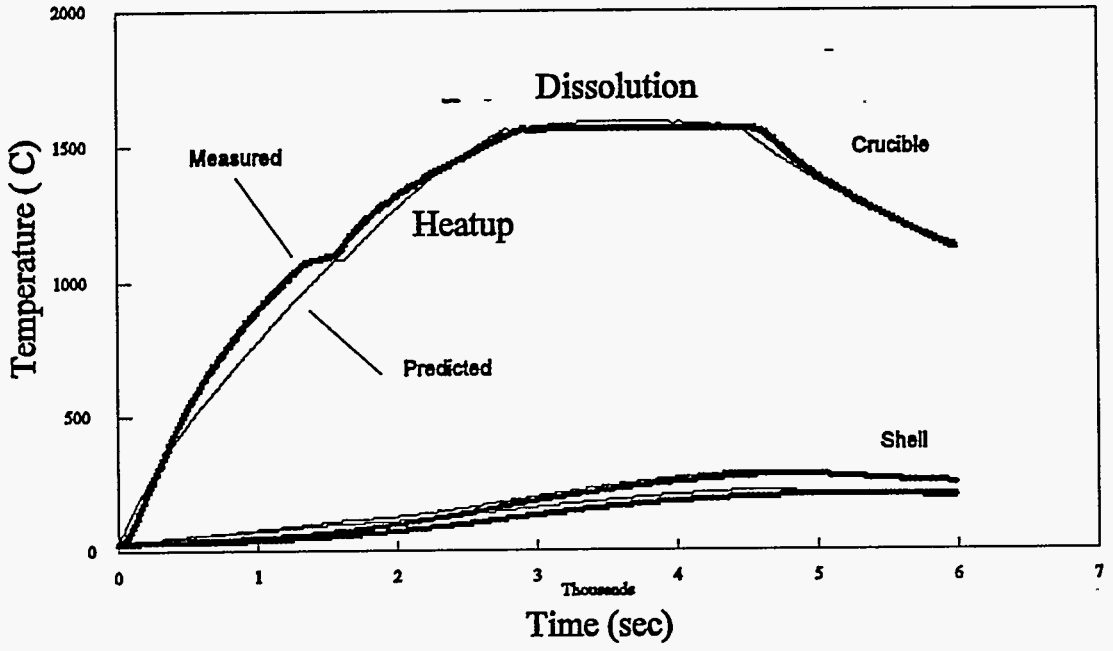

Figure 4: Comparison of the predicted and measured temperature data for a shortened depleted uranium casting. Crucible and shell temperatures.

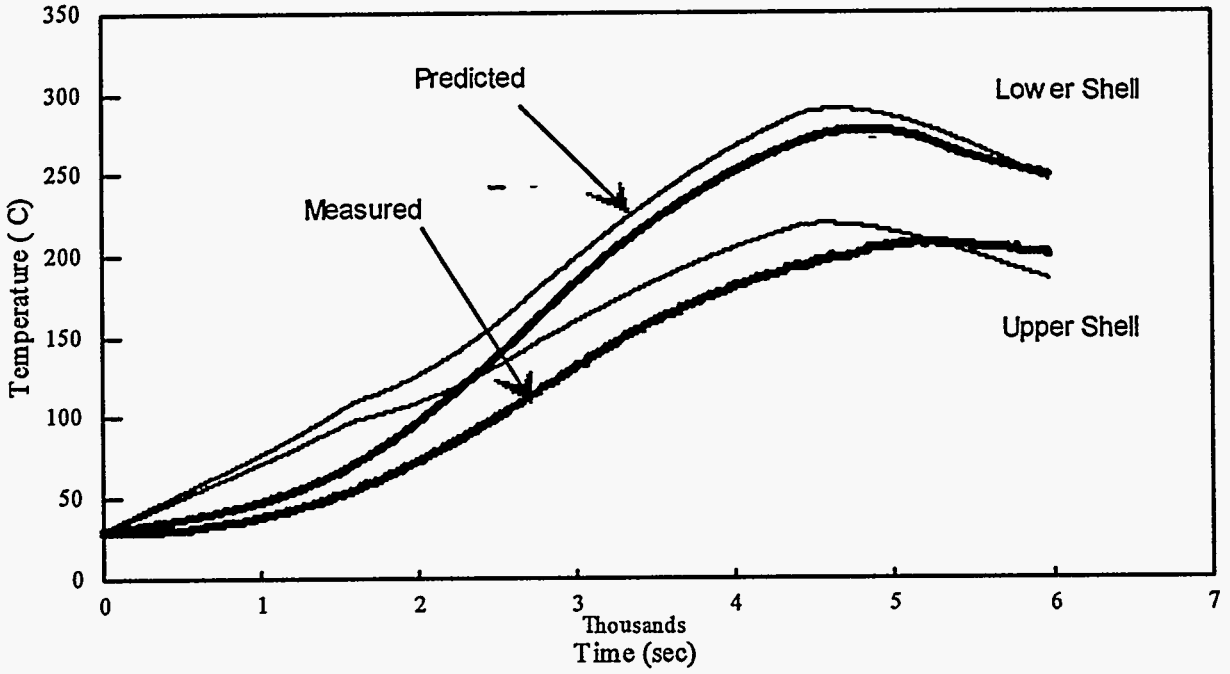

Figure 5: Comparison of the predicted and measured shell temperatures for a shortened depleted uranium casting.

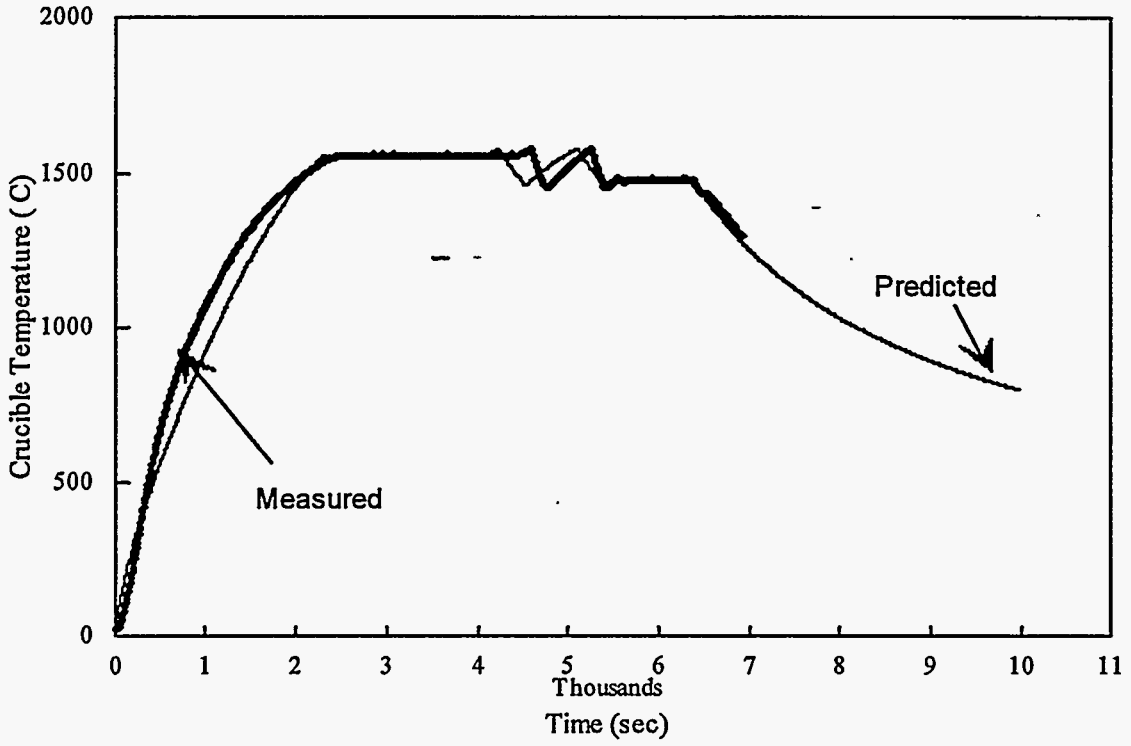

Figure 6: Comparison of the predicted and measured crucible temperature data for a depleted uranium casting.

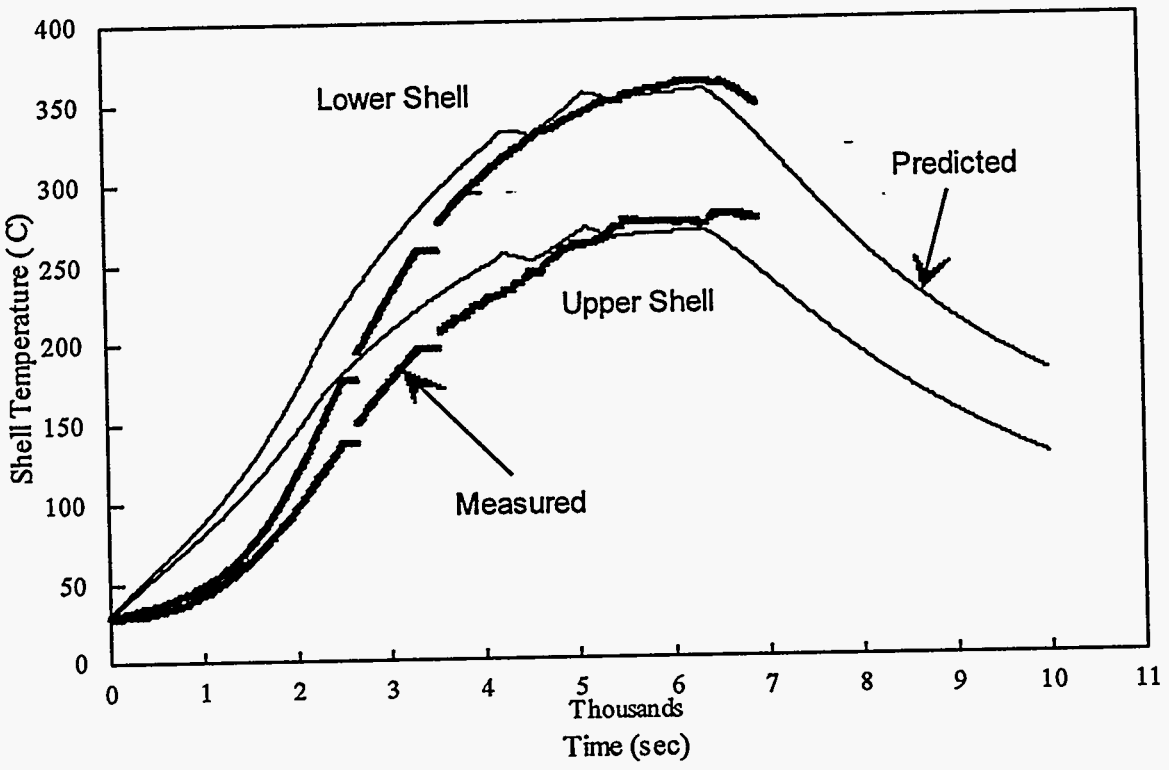

Figure 7: Comparison of the predicted and measured shell temperatures for a depleted uranium casting.

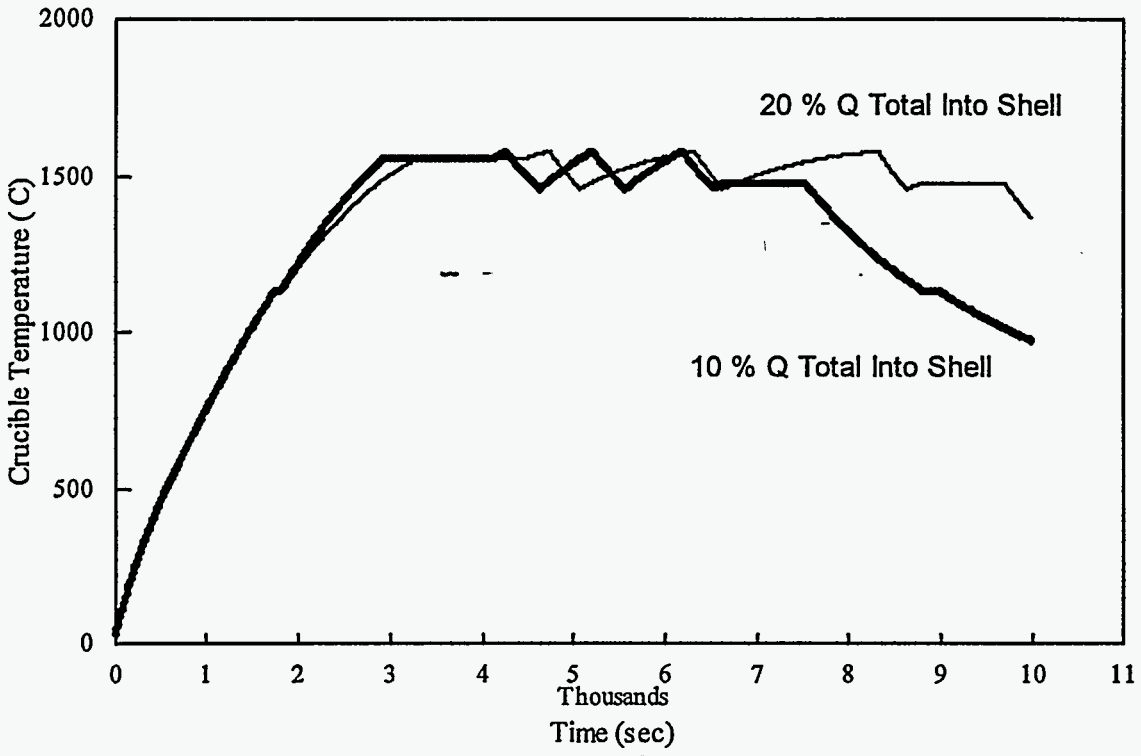

Figure 8: Effect of a 10 percent change in the amount of induction heating in the shell on the casting cycle.

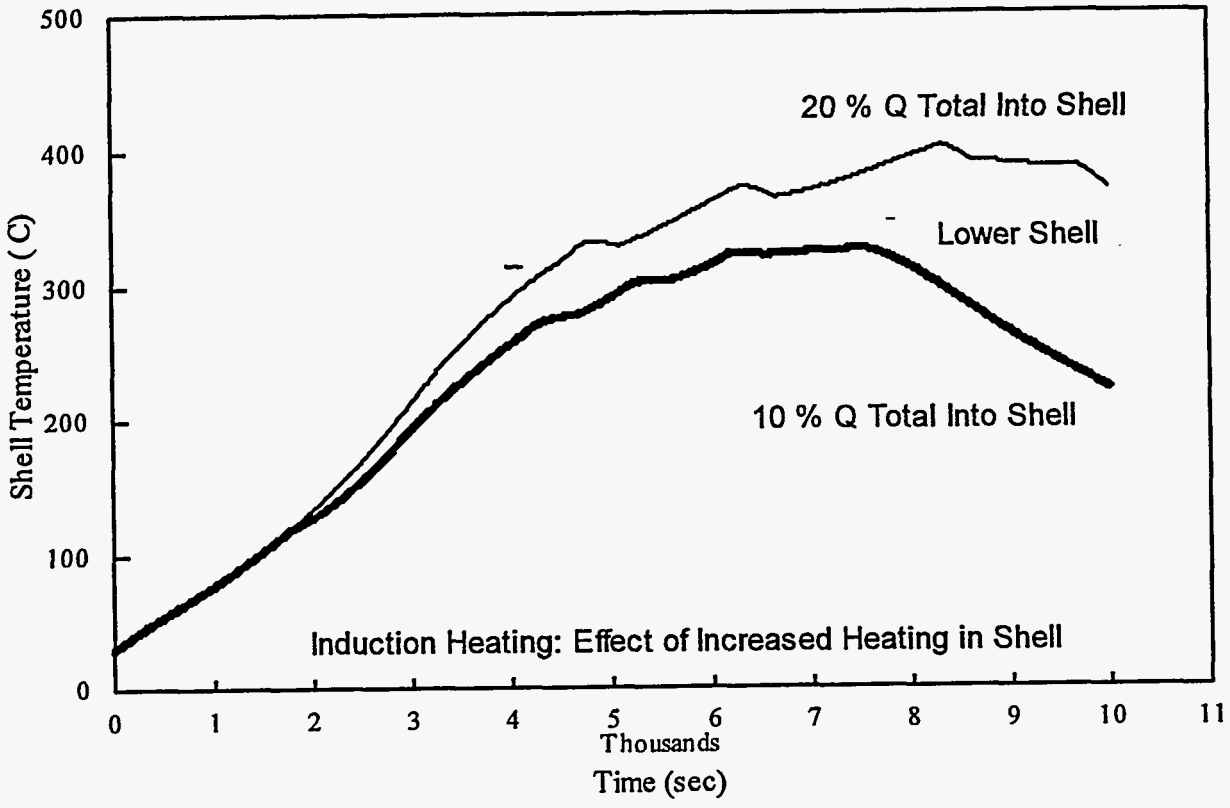

Figure 9: Effect of a 10 percent change in the amount of induction heating in the shell on the maximum shell temperature.